A new family of dinuclear lanthanide complexes exhibiting luminescence, magnetic entropy changes and single molecule magnet

Lu Dong[a], Ying-Bing Lu*[, a], Shui-Dong Zhu[c], Jun-Wei Wu[a], Xin-Ting Zhang[a], Yi Liao[a], Cai-Ming Liu*[, b], Sui-Jun Liu[c], Yong-Rong Xie[a] and Shi-Yong Zhang[a]

[a]*Jiangxi Key Laboratory of Function of Materials Chemistry, College of Chemistry and Chemical Engineering, Gannan Normal University, Ganzhou, 341000, P. R. China.*

[b]*Beijing National Laboratory for Molecular Sciences, Center for Molecular Science, Key Laboratory of Organic Solids, Institute of Chemistry, Chinese Academy of Sciences, Beijing 100190, P. R. China.*

[c]*School of Metallurgy and Chemical Engineering, Jiangxi University of Science and Technology, Ganzhou 341000, Jiangxi Province, P.R. China.*

E-mail: ybluhm@163.com, cmliu@iccas.ac.cn.

Table S1. Selected Bond Lengths (Å) for **1-4**.

Complex Eu **1**			
Eu(1)-O(1)	2.347(3)	Eu(1)-N(1)	2.572(4)
Eu(1)-O(2)A1	2.393(3)	Eu(1)-Cl(1)	2.7713(10)
Eu(1)-N(3)	2.552(4)	Eu(1)-Cl(1)A1	2.7736(11)
Eu(1)-N(4)	2.553(4)	Eu(1)-Eu(1)A1	3.9460(4)
Eu(1)-N(2)	2.564(4)		
Complex Tb **2**			
Tb(1)-O(1)	2.322(3)	Tb(1)-N(3)	2.553(3)
Tb(1)-O(2)A1	2.370(2)	Tb(1)-Cl(1)	2.7504(9)
Tb(1)-N(1)	2.526(3)	Tb(1)-Cl(1)A1	2.7491(8)
Tb(1)-N(2)	2.535(3)	Tb(1)-Tb(1)A1	3.9131(3)
Tb(1)-N(4)	2.542(3)		
Complex Gd **3**			
Gd(1)-O(1)	2.341(3)	Gd(1)-N(8)	2.562(4)
Gd(1)-O(2)A1	2.384(3)	Gd(1)-Cl(1)	2.7640(11)
Gd(1)-N(5)	2.540(4)	Gd(1)-Cl(1)A1	2.7595(10)
Gd(1)-N(6)	2.549(4)	Gd(1)-Gd(1)A1	3.9313(4)
Gd(1)-N(7)	2.551(4)		
Complex Dy **4**			

Dy(1)-O(1)	2.358(2)	Dy(1)-N(11)	2.542(3)
Dy(1)-O(2)A1	2.314(3)	Dy(1)-Cl(1)	2.7364(9)
Dy(1)-N(13)	2.525(3)	Dy(1)-Cl(1)A1	2.7415(9)
Dy(1)-N(14)	2.530(3)	Dy(1)-Dy(1)A1	3.8975(4)
Dy(1)-N(12)	2.530(3)		

Symmetry Codes for **1**, A: - *x*+1, -*y*+2, -*z*+1; For **2**, A: -*x*+1, -*y*+1, -*z*+1; For **3**, A: -*x*+1, -*y*+2, -*z*; For **4**, A: -*x*+2, -*y*-1, -*z*.

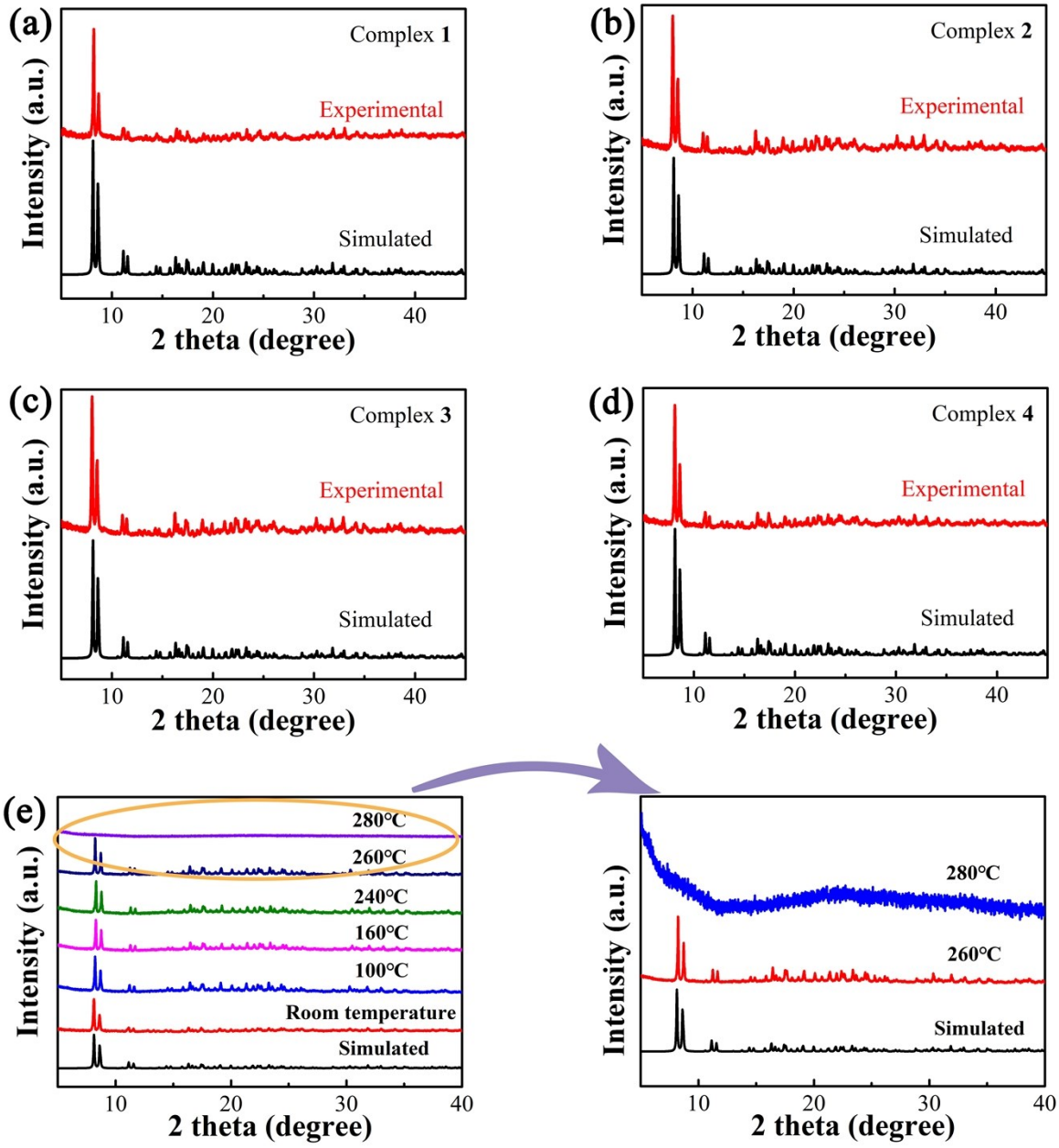

Figure S1. Powder X-ray diffraction patterns of **1** (a), **2** (b), **3** (c) and **4** (d), and the variable-temperature PXRD patterns of complex **4** (e)

Table S2. Summary of SHAPE analysis for **4.**

label	shape	symmetry	Distortion(τ)
OP-8	Octagon	D_{8h}	18.163
HPY-8	Heptagonal pyramid	C_{7v}	15.308
HBPY-8	Hexagonal bipyramid	D_{6h}	21.227
CU-8	Cube	O_h	27.501
SAPR-8	Square antiprism	D_{4d}	21.276
TDD-8	Triangular dodecahedron	D_{2d}	22.005
JGBF-8	Johnson gyrobifastigium J26	D_{2d}	17.894
JETBPY-8	**Johnson elongated triangular bipyramid J14**	$\mathbf{D_{3h}}$	**14.393**
JBTPR-8	Biaugmented trigonal prism J50	C_{2v}	17.876
BTPR-8	Biaugmented trigonal prism	C_{2v}	18.496
JSD-8	Snub diphenoid J84	D_{2d}	19.911
TT-8	Triakis tetrahedron	T_d	27.509
ETBPY-8	Elongated trigonal bipyramid	D_{3h}	15.380

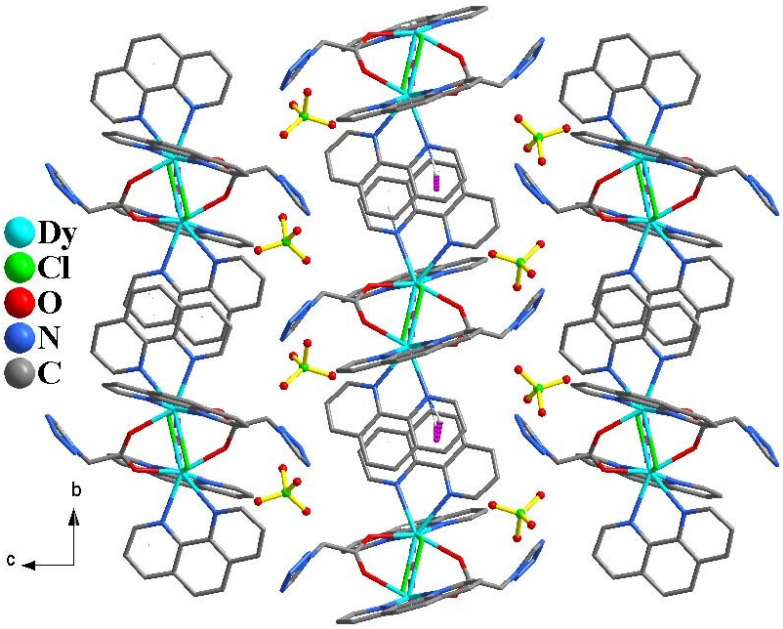

Figure S2. The counteranions $[ClO_4]^-$ lying between the layers along the *bc* plane in **4**.

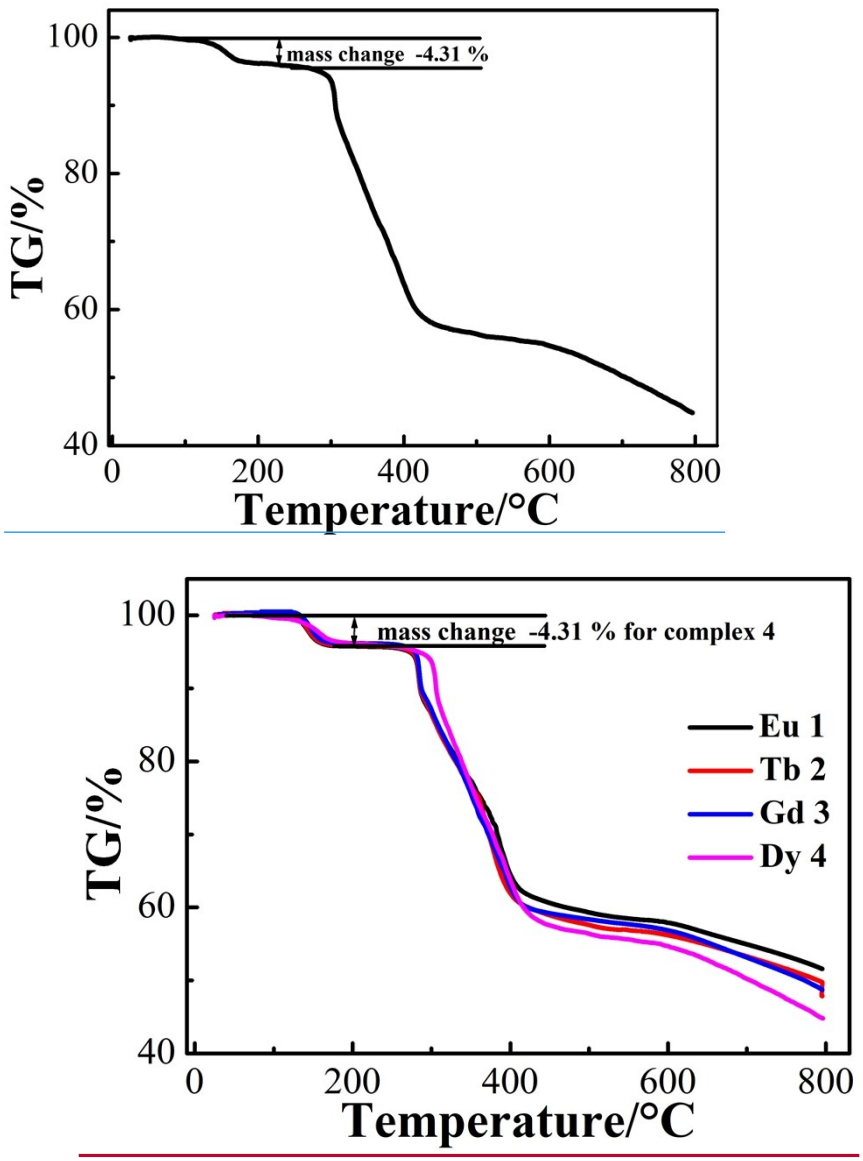

Figure S3. The TGA plot of **1-4**.

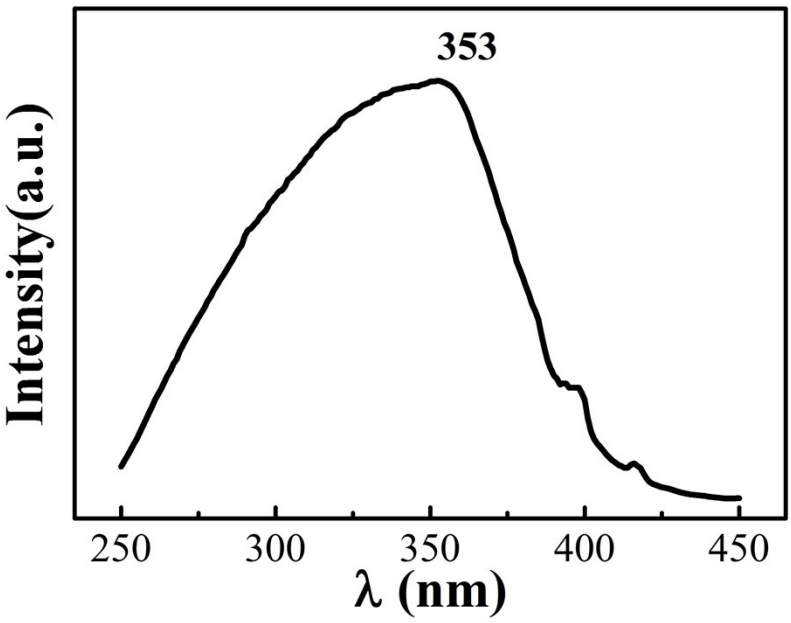

Figure S4. Solid-state excitation spectra at room temperature for **1**.

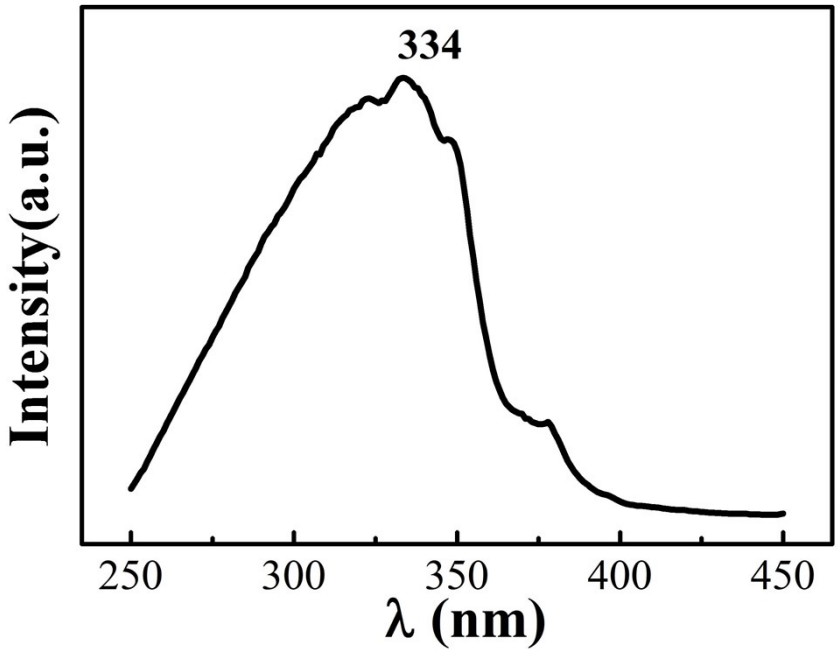

Figure S5. Solid-state excitation spectra at room temperature for **2**.

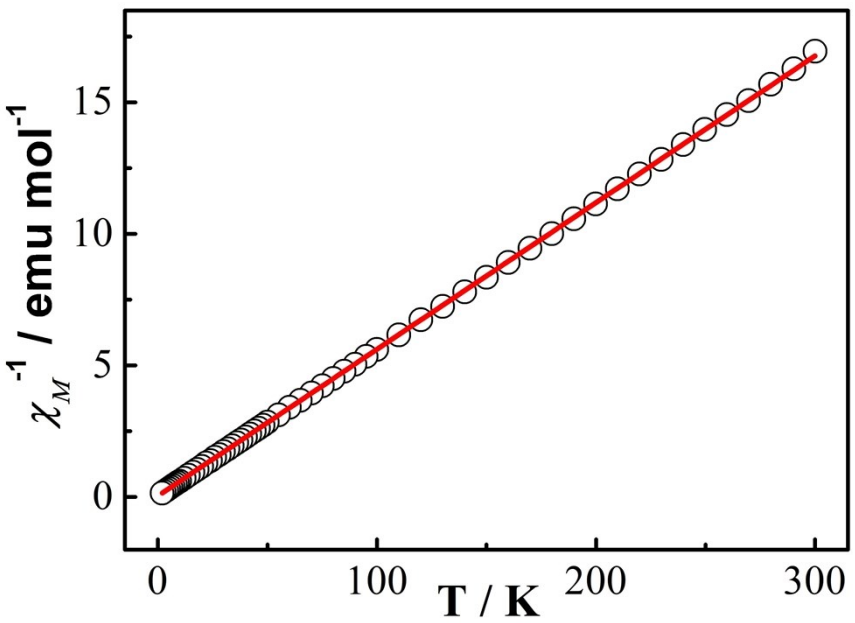

Figure S6. Temperature evolution of the inverse magnetic susceptibility for **3** between 2 and 300 K.

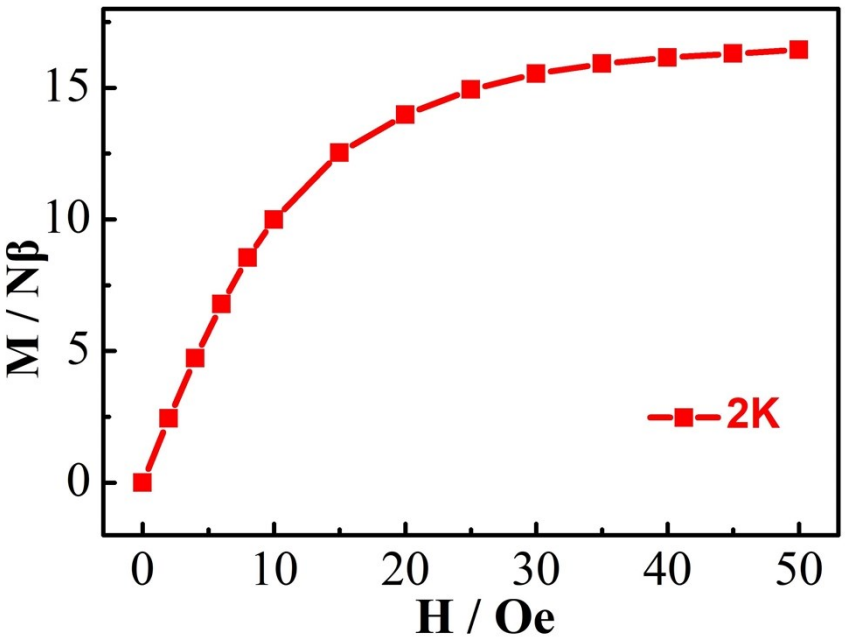

Figure S7. The *M vs*. *H* plot for 0–5 T at 2 K for **3**.

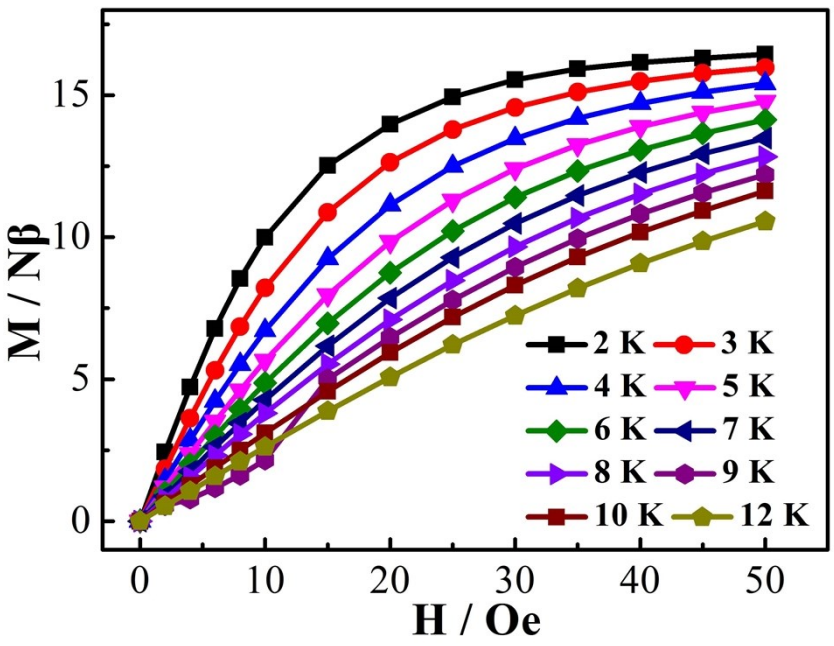

Figure S8. The *M* vs *H* curves of 3 at *T* = 2-12 K and *H* = 0-50 kOe for **3**.

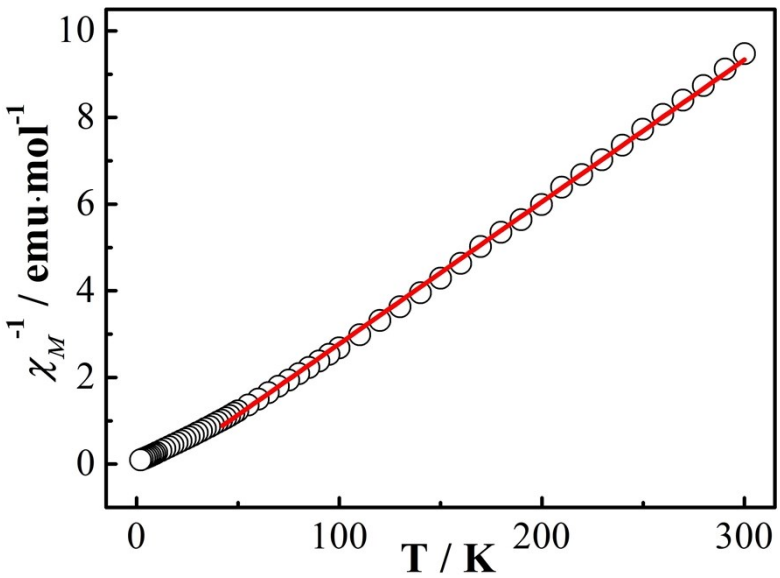

Figure S9. Temperature evolution of the inverse magnetic susceptibility for **4** between 40 and 300 K.

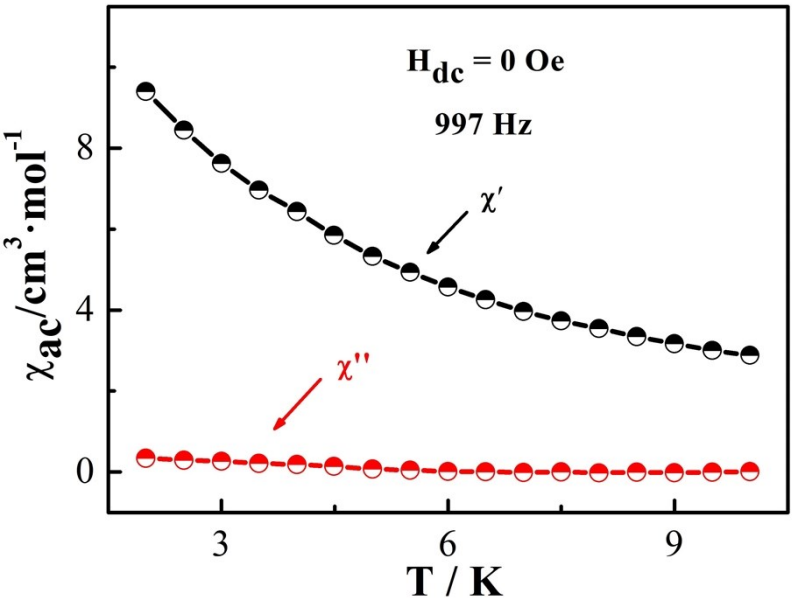

Figure S10. ac susceptibility measurements at frequency with 977 Hz for **4** at H_{dc} = 0 Oe, H_{ac} = 2.5 Oe.

Table S3. Linear combination of two modified Debye model fitting parameters from 2 and 2.5 K of **4** under 1000 Oe dc field.

T (K)	τ_1 (s)	α_1	τ_2 (s)	α_2
2	0.000279378	0.223	0.00467199	0.019
2.5	0.000155311	0.186	0.00238555	0.030

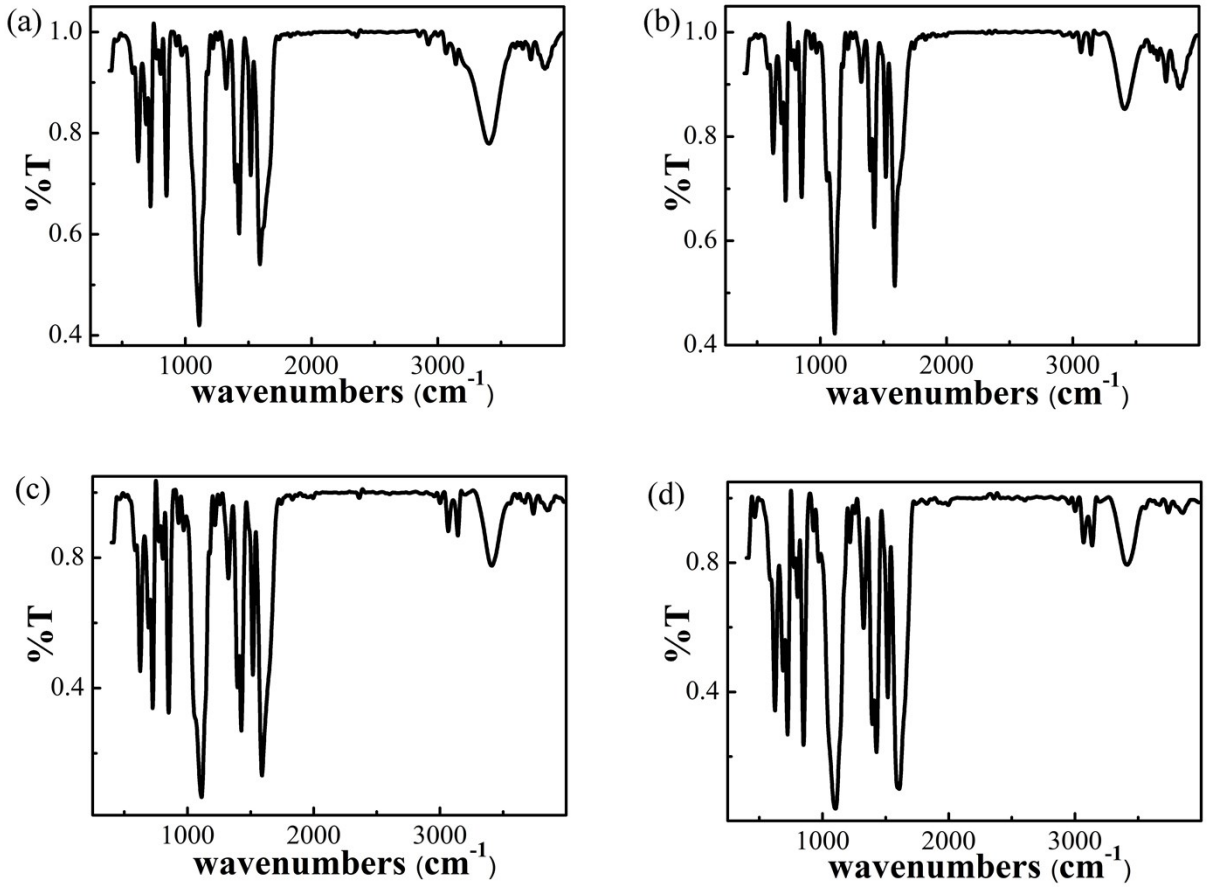

Figure S11. IR spectra for **1** (a), **2** (b), **3** (c) and **4** (d).